Supplementary Information

Photo-Fenton Degradation of Ciprofloxacin Over Cu, Ce co-doped Monoclinic $BiVO_4$ Photocatalyst

*Nivedita Singh, and Indrajit Sinha**

Department of Chemistry, Indian Institute of Technology (Banaras Hindu University), Varanasi 221005, India

*Corresponding author email: isinha.apc@iitbhu.ac.in

S1 Materials Used

All reactants and chemicals used in the present research were of analytical grade. Out of these, bismuth nitrate pentahydrate $Bi(NO_3)_3.5H_2O$ (≥ 99%) and cupric acetate monohydrate $(CH_3COO)_2Cu.H_2O$ (≥ 98%), NH_4OH (25 vol%) were purchased from Merck. Cerous nitrate hexahydrate $Ce(NO_3)_3.6H_2O$ (≥ 99%) was purchased from SRL chemicals. Ammonium metavanadate (NH_4VO_3) (≥ 99%) and ciprofloxacin were purchased from HIMEDIA.

S2 Characterization techniques

The X-ray diffraction (XRD) patterns of all powdered samples were recorded on a Rigaku Miniflex 600 diffractometer (Rigaku Corporation, Japan) using Cu Kα radiation (λ = 1.54056 Å), with a scan rate of 5° min^{-1} and a step size of 0.01°. High Score Plus software (Malvern Panalytical, 2011), with the ICSD database, was used to perform phase identification from all the powder XRD data. High-resolution / Field emission scanning electron microscopy (HR/FE-SEM) images were obtained on a Nova NanoSEM 450 (FEI, USA), and energy dispersive spectroscopy (EDS) for elemental mapping was performed using a Team Pegasus Integrated EDS-EBSD system with

Octane Plus and Hikari Pro detectors (EDAX Inc., USA). High resolution transmission electron microscopy (HR-TEM) images were recorded on a Tecnai G2 20 TWIN (FEI company) equipped with the operated voltage of 200 keV. The solid-state photoluminescence (PL) spectra were recorded using a Witec Alpha 300 RAS spectrometer equipped with a 405 nm pulsed diode laser (5.49 mW). The Raman spectra of all samples were obtained with an STR300 micro-Raman spectrophotometer, utilizing a 532nm laser (1mW power). The UV–visible absorbance spectra of liquid samples were measured using an Agilent Cary-60 spectrophotometer, while solid-state UV diffuse reflectance spectroscopy (UV-DRS) was carried out on a Shimadzu UV-2600 to estimate the optical band gap. X-ray photoelectron spectroscopy (XPS) measurements were performed on a K-Alpha spectrometer (Thermo Fisher Scientific) to analyze surface composition, oxidation states, and the valence band maximum.

S3 Electrochemical Impedance Spectroscopy (EIS) and Photocurrent Measurements

EIS measurements were performed with a Metrohm Autolab M204 electrochemical workstation. All electrochemical measurements were carried out in a single-compartment photoelectrolytic cell having 25 mL electrolyte (0.5 M phosphate buffer solution with pH 7) with the photoanode@FTO as the working electrode, Ag/AgCl as the reference electrode, and Pt wire as the counter electrode. Electrochemical impedance spectroscopic (EIS) measurements were carried out in the frequency range of 0.001 to 100,000 Hz with an amplitude of 20 mV in the dark and light. A Xenon lamp 1 Sun was used as the light source. The pure and doped BVO Samples were dropcast on a 1 × 1 cm^2 FTO glass electrode using Nafion as a binder. The photocurrents of the samples were also measured via the same methods.

S4 Recyclability experiment details

Recyclability experiments were conducted to assess the catalyst's photostability. For that, 20 mg catalyst was dispersed in 30 mL of 10 ppm CIP solution at pH~3 and sonicated for 30 min. The reaction mixture was placed in the dark for 1 hour for the adsorption-desorption equilibrium. After that, 400µl H_2O_2 (The optimization of H_2O_2 concentration in this process was performed by scaling the volume of 0.5M H_2O_2 in direct proportion to the volume of 10 ppm CIP used in the optimization procedure outlined in Photo-Fenton activity for CIP degradation section, ensuring the same molar ratio between H_2O_2 and CIP is maintained) was then added to the reaction mixture. The reaction mixture was placed in a cool white LED light chamber for 120 min, and the UV-Visible absorbance of the aliquot was recorded.

S5 Rietveld refined plot of pure and doped BVO samples

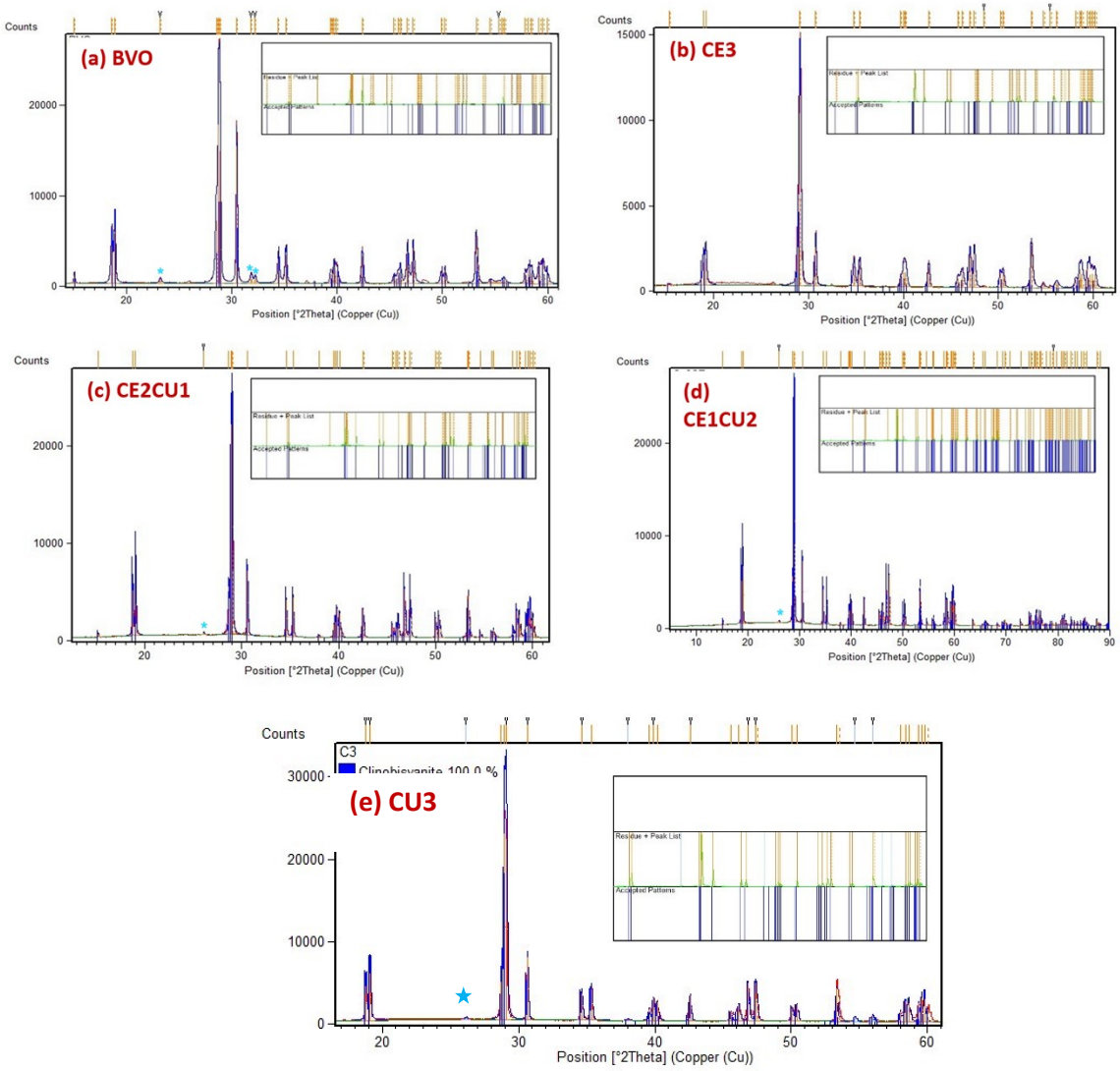

Figure S1 Rietveld refinement plot of (a) BVO, (b) CE3, (c) CE2CU1, (d) CE1CU2, (e) CU3

S6 HR-SEM images of pure and doped BVO samples

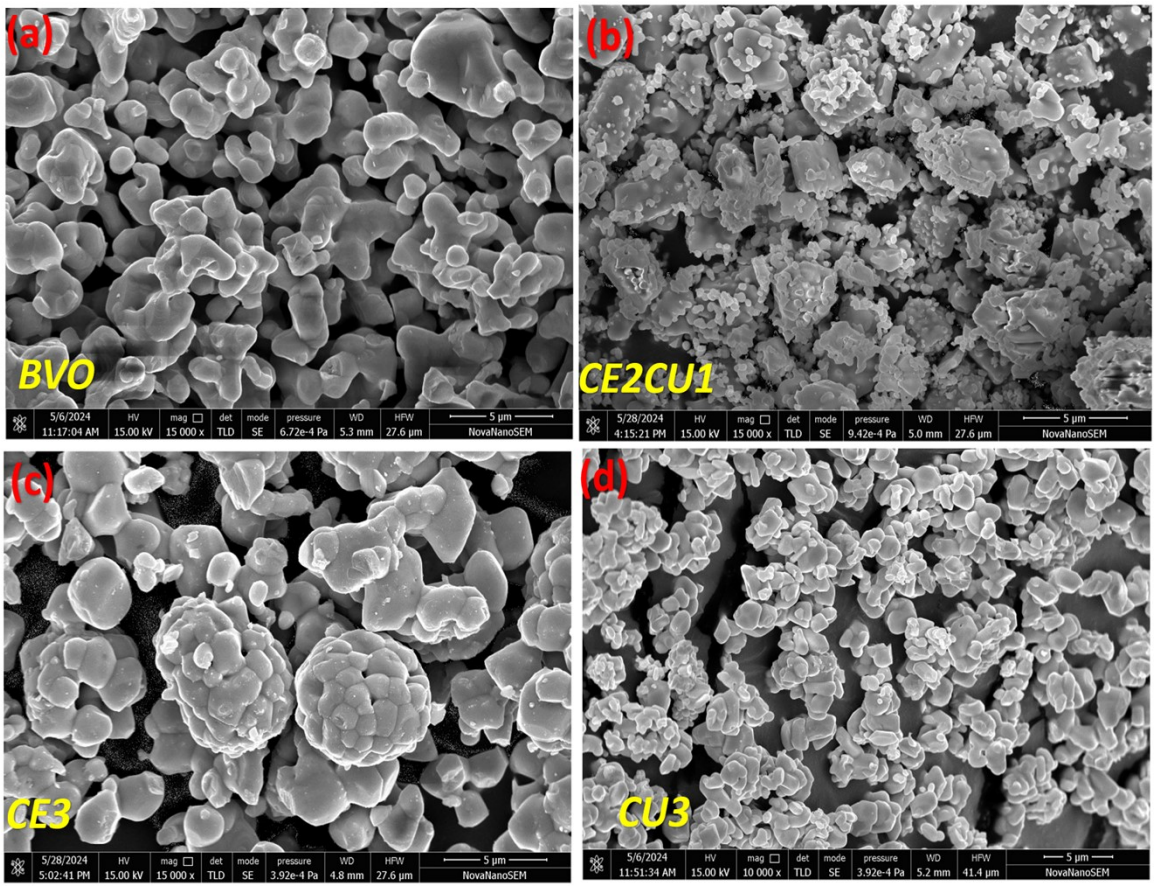

Figure S2 HR-SEM micrographs of (a) BVO, (b) CE2CU1, (c) CE3, (d) CU3

S7 Deconvoluted HR-XPS of recycled CE1CU2 sample

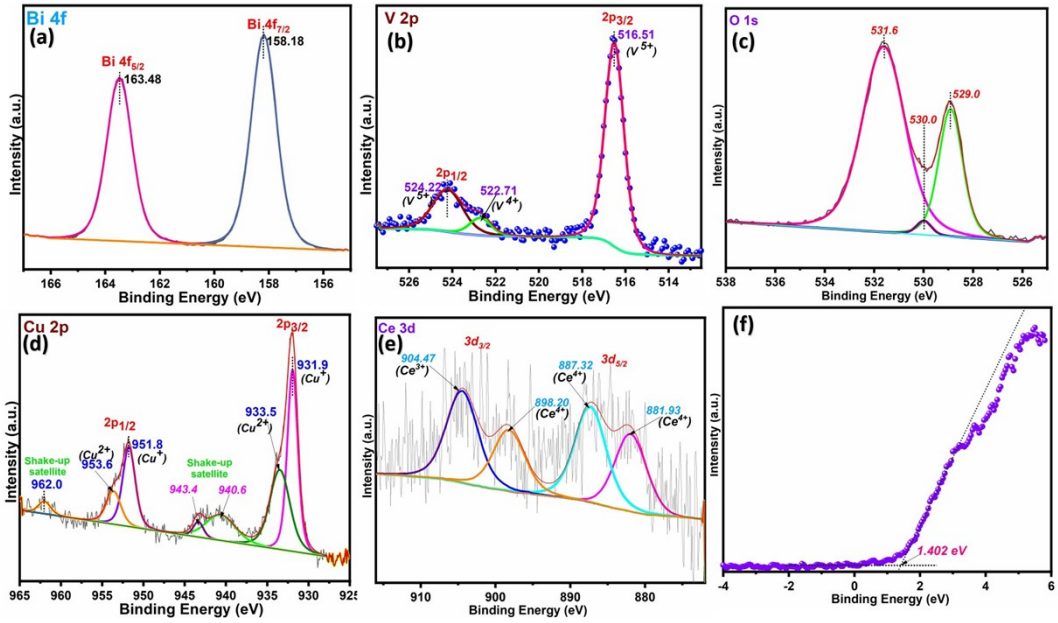

Figure S3 HR-XPS of (a) Bi4f, (b) V2p, (c) O1s, (d) Cu2p & (e) Ce3d, (f) valence band (VB) spectra of CE1CU2 sample after five cycles of use.

S8 Cu 2p HR- XPS of CU3 sample

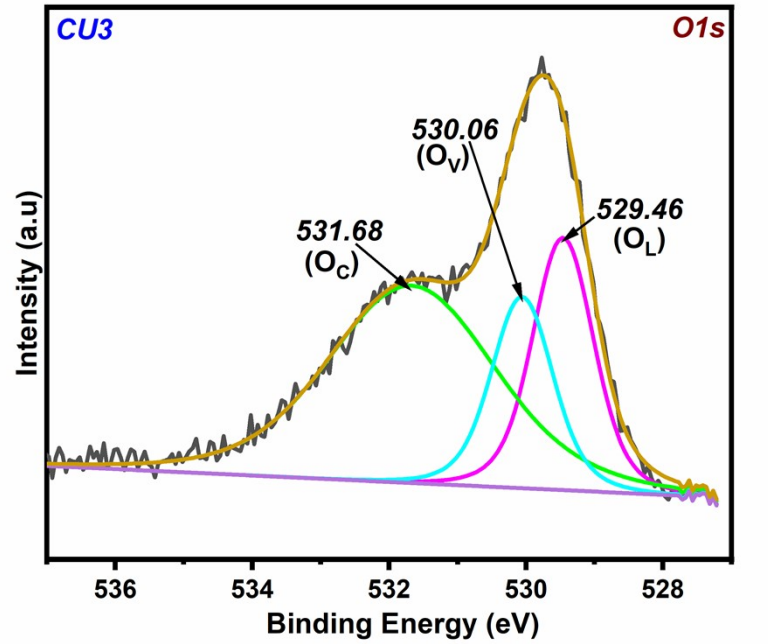

Figure S4 Deconvoluted O1s HR-XPS of CU3 sample

S9 Photocatalytic CIP degradation without H_2O_2

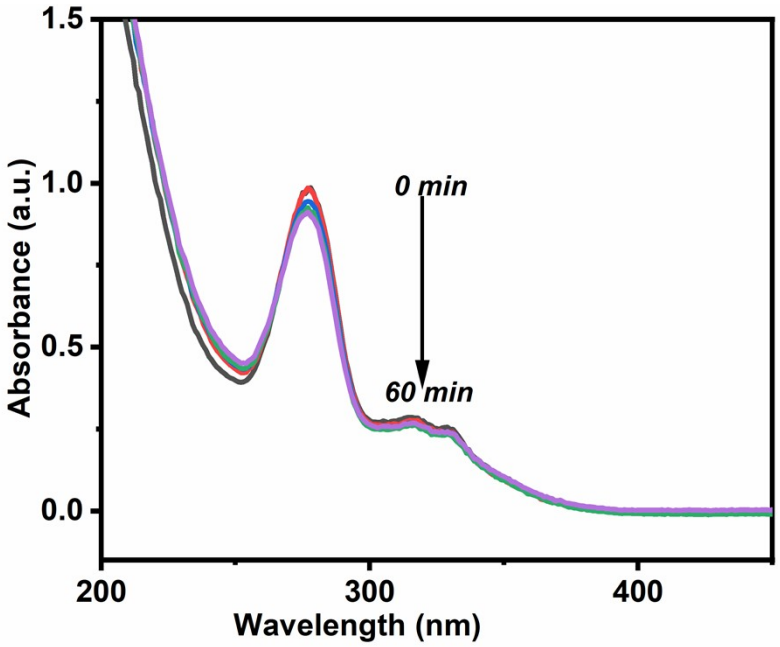

Figure S5 Photocatalytic CIP degradation without H_2O_2 in 60 min of light irradiation

S9 Effect of pH and H_2O_2 amount variation on the Photo-Fenton CIP degradation

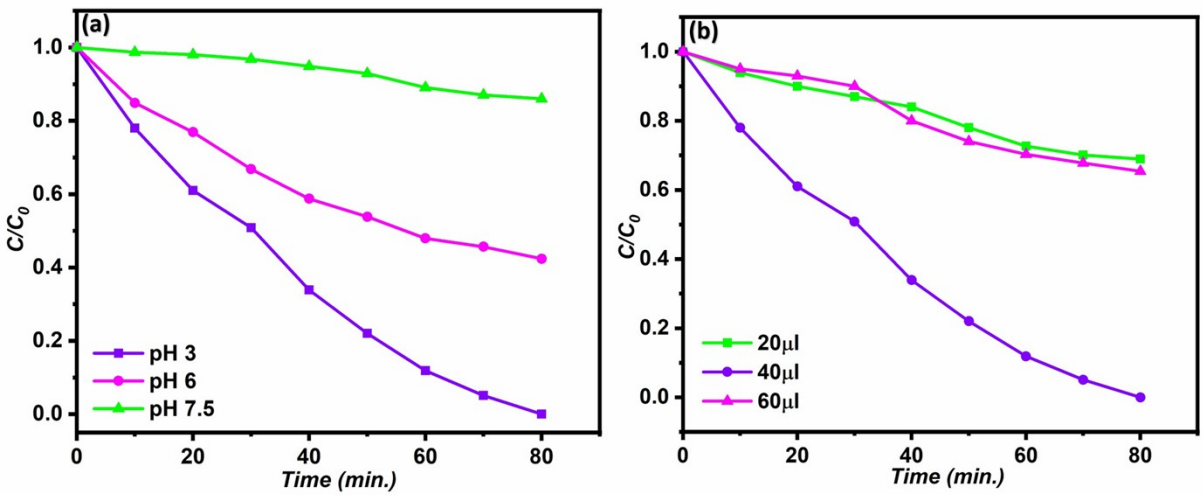

Figure S6 Effect of (a) pH variation, and (b) H_2O_2 amount variation on the Photo-Fenton CIP degradation.

S10 Transient photocurrent response

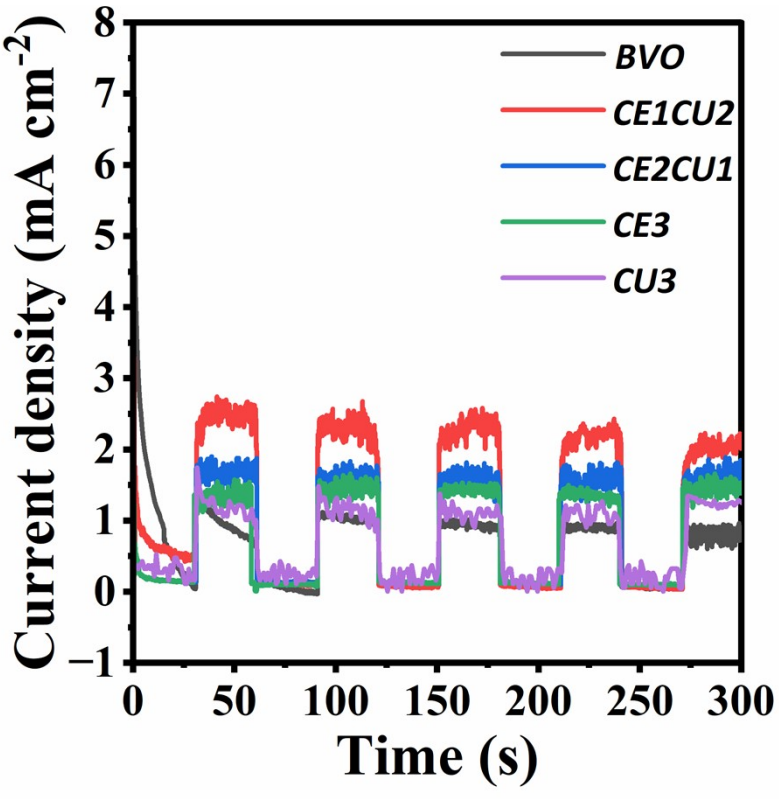

Figure S7 Photocurrent response at 1.23 V vs. RHE for all the photoanodes

Table S1. The calculated lattice parameter values of BVO and doped samples using XRD data

Sample	**a (Å)**	**b (Å)**	**c (Å)**	**β (°)**	**V (Å³)**
Reference (JCPDS #14-0688)	5.19	11.70	5.09	90.38	309.52
BVO	5.20	11.71	5.07	89.93	310.76
CE3	5.15	11.62	5.10	90.92	303.39
CE2CU1	5.18	11.67	5.08	90.29	307.48
CE1CU2	5.15	11.60	5.06	91.03	302.42
CU3	5.18	11.68	5.07	90.57	306.75

Table S2. Refined lattice parameters from Rietveld refinement

Sample	**BVO**	**CE3**	**CE2CU1**	**CE1CU2**	**CU3**
a (Å)	5.14	5.16	5.14	5.13	5.18
b (Å)	11.70	11.71	11.72	11.70	11.75
c (Å)	5.10	5.12	5.11	5.12	5.13
β (°)	90.34	90.34	90.36	90.39	90.42

Table S3. Comparative band gaps (E_g) of pure and doped BVO samples by absorbance plot, direct and indirect Tauc plots

Sample	**Abs. plot (eV)**	**Indirect E_g (eV)**	**Direct E_g (eV)**
BVO	2.38	2.23	2.45
CE3	2.16	1.81	2.35
CE2CU1	2.40	2.25	2.49
CE1CU2	2.49	2.40	2.55
CU3	2.42	2.35	2.48

Table S4. Raman frequency values for the symmetric stretching $\nu_s(V-O)$, asymmetric stretching $\nu_{as}(V-O)$, symmetric bending $\delta_s(VO_4)^{3-}$, asymmetric bending $\delta_{as}(VO_4)^{3-}$, and external modes

Specimen	**BVO**	**CE3**	**CE2CU1**	**CE1CU2**	**CU3**
$\nu_s(V-O)$	827.6	824.9	826.5	827.5	823.9
$\nu_{as}(V-O)$	751.1	737.1	750.3	747.7	746.5
$\delta_s(VO_4)^{3-}$	367.2	366.4	366.8	367.0	365.0
$\delta_{as}(VO_4)^{3-}$	323.9	325.6	325.3	324.6	322.8
external modes	209.1	209.1	209.3	209.5	206.3

Table S5. Atomic percentage of Bi, V, O, Cu, and Ce in BVO, fresh and reused CE1CU2 samples' XPS survey spectra

Sample	**Bi 4f**	**V 2p**	**O 1s**	**Cu 2p**	**Ce 3d**
BVO	30.39	5.50	64.11	-	-
Fresh CE1CU2	26.84	6.22	66.06	0.51	0.38
Reused CE1CU2	26.86	6.28	66.41	0.33	0.12

Table S6. Atomic percentage of Cu and Ce in the deconvoluted Fresh and reused CE1CU2 samples' XPS spectra

Element	Fresh CE1CU2		Reused CE1CU2	
	Binding Energy (eV)	Atomic Percentage	Binding Energy (eV)	Atomic Percentage
Cu2p	932.0	45.43	931.9	31.63
	951.8	18.72	951.8	26.36
	933.8	14.27	933.5	16.68
	953.6	6.72	953.6	7.92
Ce3d	880.2	27.27	881.93	22.87
	883.9	31.64	887.32	29.64
	898.5	10.28	898.20	19.02
	902.2	30.81	904.47	28.46

Table S7. Comparative TOF and H-TOF data for the prepared catalyst and the previously published copper-based photo-Fenton catalysts for CIP degradation

Catalyst	Reaction Conditions	Degradation efficiency	TOF (μmoles g^{-1} min^{-1})	H-TOF (10^{-6} mg^{-1} min^{-1} L)	Reference
$(Cu_3(PO_4)_2)$	100 mL, 15 ppm CIP 25 mg catalyst 50μL, 30% H_2O_2 200W Hg-Xe lamp	100% in 6h	5.03	1.02	[1]
$Cu_2(OH)_3F$/CQDs-$BiVO_4$	50 mL, 20 ppm CIP 10 mg catalyst 200μL, 0.4g/L H_2O_2	98.1% in 1h	493.36	10.5×10^3	[2]
α- (Fe, Cu) OOH/RGO	50 mL, 30 ppm CIP 0.40 g/L catalyst 0.15 M H_2O_2 Visible light	99% in 180 min.	124.5	0.83	[3]
Sodium Alginate hydrogel/Cu@MoS_2/CNF@CDs	250 mL, 20 ppm CIP 80 mg catalyst 6 mM H_2O_2 Visible light	96.7% in 100 min.	182.28	30.4	[4]

Ultrathin CuZnCr-LDH nanosheets	50 mL, 50 ppm CIP 25 mg catalyst 1mL H_2O_2 300W Xe lamp (UV)	75% in 3h	125.73	*	[5]
CA-Cu/TCN	30 mL, 20 ppm CIP 0.5 g/L catalyst 68 mM H_2O_2 300 W Xe lamp (Visible light)	95.1% in 60 min.	191.3	2.81	[6]
Cu-C_3N_4	50 mL, 10 ppm CIP 20 mg catalyst 3 mL H_2O_2 (30%) 300 W Xe lamp (Visible light)	99% in 30 min.	247.5	0.42	[7]
UNH(Zr/Fe)@CuO-25	100 mL, 10 ppm CIP 10 mg catalyst 0.2 mL H_2O_2 300 W Xe lamp (Visible light)	80.1% in 60 min.	402.83	*	[8]
$CuCOFe_2O_4$@AC	200 mL, 15 ppm CIP 600mg/L catalyst 2500mg/L H_2O_2 6W UV lamp	84% in 50 min.	126.73	1.72	[9]
Cu, Mn co-doped $BiVO_4$	3 mL, 10 ppm CIP 500µLcatalyst (1mg/mL) 40µL, 0.5M H_2O_2	100% in 100 min.	211.2	36.96	[10]
CE1CU2	3 mL, 10 ppm CIP 500µLcatalyst (1mg/mL) 40µL, 0.5M H_2O_2	~100% in 80 min.	264.0	46.20	Present article

*data reported is inadequate for calculation

References

1 M. Rozmyślak, A. Walkowiak, M. Frankowski and L. Wolski, *Sci. Rep.*, DOI:10.1038/s41598-024-57542-9.

2 X. Zhang, Y. Liu, Y. Zhai, Y. Yu, Y. Guo and S. Hao, *Environ. Res.*, 2023, **222**, 115347.

3 J. Xu, D. Hu, Y. Wang and Z. Zhang, *Environ. Sci. Pollut. Res.*, 2022, **29**, 78874–78886.

4 J. Ouyang, W. Lv, C. Wang, X. Guo, H. Lv and Y. Wu, *Chem. Eng. J.*, 2025, **520**, 166277.

5 Z. He, T. Shi, D. Chen, Y. Wang, Y. Feng, F. Zhou and Y. Li, *J. Alloys Compd.*, 2025, **1010**, 177302.

6 R. Huang, D. Liang, W. Zhang, T. Gan, H. Hu, Z. Huang and Y. Zhang, *J. Colloid Interface Sci.*, 2025, **678**, 987–1000.

7 S. Dong, X. Chen, L. Su, Y. Wen, Y. Wang, Q. Yang, L. Yi, W. Xu, Q. Yang, P. He, Y. Zhu and Z. Lu, *ACS ES T Eng.*, 2023, **3**, 150–164.

8 H. H. Haitosa, L. He, P. Chen, D. M. Kabtamu, O. A. Zelekew and Y. nan Wu, *J. Environ. Chem. Eng.*, 2025, **13**, 120296.

9 M. Pourshaban-Mazandarani, M. Ahmadian, A. Nasiri and A. Poormohammadi, *Appl. Water Sci.*, 2023, **13**, 1–18.

10 N. Singh and I. Sinha, *Langmuir*, 2025, **41**, 14935–14945.